Article No. jmbi.1999.3205 available online at http://www.idealibrary.com on IDEAL® J. Mol. Biol. (1999) 293, 1121–1132

JMB

Structure Determination of the Glutamate Dehydrogenase from the Hyperthermophile *Thermococcus litoralis* and its Comparison with that from *Pyrococcus furiosus*

K. L. Britton[1], K. S. P. Yip[1], S. E. Sedelnikova[1], T. J. Stillman[1] M. W. W. Adams[3], K. Ma[3], D. L. Maeder[2], F. T. Robb[2], N. Tolliday[2] C. Vetriani[2], D. W. Rice[1]* and P. J. Baker[1]

[1]*The Krebs Institute for Biomolecular Research Department of Molecular Biology and Biotechnology University of Sheffield Sheffield S10 2TN, UK*

[2]*Center of Marine Biotechnology, University of Maryland Biotechnology Institute, 701 E. Pratt Street Baltimore, MD 21202, USA*

[3]*Department of Biochemistry and Molecular Biology University of Georgia, Athens GA 30602, USA*

**Corresponding author*

Glutamate dehydrogenase catalyses the oxidative deamination of glutamate to 2-oxoglutarate with concomitant reduction of $NAD(P)^+$, and has been shown to be widely distributed in nature across species ranging from psychrophiles to hyperthermophiles. Extensive characterisation of this enzyme isolated from hyperthermophilic organisms has led to its adoption as a model system for analysing the determinants of thermal stability. The crystal structure of the extremely thermostable glutamate dehydrogenase from *Thermococcus litoralis* has been determined at 2.5 Å resolution, and has been compared to that from the hyperthermophile *Pyrococcus furiosus*. The two enzymes are 87% identical in sequence, yet differ 16-fold in their half-lives at 104 °C. This is the first reported comparative analysis of the structures of a multisubunit enzyme from two closely related yet distinct hyperthermophilies. The less stable *T. litoralis* enzyme has a decreased number of ion pair interactions; modified patterns of hydrogen bonding resulting from isosteric sequence changes; substitutions that decrease packing efficiency; and substitutions which give rise to subtle but distinct shifts in both main-chain and side-chain elements of the structure. This analysis provides a rational basis to test ideas on the factors that confer thermal stability in proteins through a combination of mutagenesis, calorimetry, and structural studies.

Keywords: crystal structure; glutamate dehydrogenase; protein stability; *Thermococcus litoralis*; *Pyrococcus furiosus*

Introduction

The ability of enzymes from hyperthermophiles to operate for long periods at temperatures in excess of 100 °C has prompted much research into the molecular mechanisms that give rise to such remarkable properties (Flam, 1994). Analysis of the structure of hyperthermophilic proteins has highlighted a range of differences between these enzymes and their mesophilic counterparts, including increased numbers of ion pairs, reduction in the size of loops and in the number of cavities, reduced ratio of surface area to volume, introduction of additional proline residues, increased hydrophobic interaction at subunit interfaces, increase in the extent of secondary structure formation and truncated N and C termini (Elcock, 1998; Vogt *et al.*, 1997; Tanner *et al.*, 1996; Starich *et al.*, 1996; Yip *et al.*, 1995; Chan *et al.*, 1995; Korndörfer *et al.*, 1995; Russell *et al.*, 1994). Some of these hypotheses have been tested by mutagenesis and recent work has indicated that increments of stability may be achieved in proteins from mesophiles by a variety of mechanisms such as the inclusion of ''rigidifying'' mutations to flexible regions of secondary structure and the introduction of charged-charged interactions (Van Den Burg *et al.*, 1998; Bogin *et al.*, 1998; Zhang *et al.*, 1995).

Abbreviations used: *Pf*, *P. furiosus*; *Tl*, *T. litoralis*; GluDH, glutamate dehydrogenase; *Cs*, *C. symbiosum*.

E-mail address of the corresponding author: d.rice@sheffield.ac.uk

0022-2836/99/451121–12 $30.00/0

The changes in stabilisation energy required to adapt an enzyme to high temperature operation are thought to be only of the order of a few hydrogen bonds, van der Waals contacts or stabilising ion pairs (Jaenicke, 1996). That no generally accepted unifying theory on the origins of stability has yet emerged may well be due to the different ways in which nature can produce such subtle effects. The fact that this energy difference is so small highlights the difficulties associated with understanding the molecular basis of this phenomena, even where high resolution crystal structures are available.

Pyrococcus furiosus (*Pf*) and *Thermococcus litoralis* (*Tl*) are hyperthermophilic organisms whose optimal growth temperatures are 100 °C (Fiala & Stetter, 1986) and 88 °C (Neuner *et al*., 1990), respectively. The glutamate dehydrogenases (GluDH, EC 1.4.1.2-4) from these organisms are closely related sharing 87 % sequence identity with only a single residue insertion between the two sequences. Despite this similarity, the *Pf* enzyme has a half life of 4.6 hours at 104 °C compared with 0.3 hour for the *Tl* enzyme with their melting temperatures being 114.5 °C and 109 °C, respectively (Vetriani *et al*., 1998). Following the determination of the structure of the *Pf* GluDH (Yip *et al*., 1995), we have sought to crystallise and examine the structure of the corresponding *Tl* enzyme. Here we report the structure determination of *Tl* GluDH at 2.5 Å, and its comparison to the *Pf* GluDH structure as a contribution towards a better understanding of factors controlling stability.

Results

Throughout this paper the *Pf* GluDH numbering is used when identifying equivalent residues in the *Tl* enzyme. In each case, when referring to positions of sequence difference between the two enzymes a bold italic style is used and the residue in *Pf* GluDH is identified first (e.g. ***I107V***). Elsewhere, the notation D167T, for example, in normal type, is used to describe the creation of a mutant enzyme by site-directed mutagenesis with the residue in the wild-type enzyme first.

Molecular structure

The molecular structure of *Tl* GluDH is very similar to that seen in all the other GluDHs whose structures have been elucidated, which include those from *Clostridium symbiosum* (*Cs*) (Baker *et al*., 1992), *Escherichia coli* (Abeysinghe, 1993), *Thermotoga maritima* (Knapp *et al*., 1997) and *Pyrococcus furiosus* (Yip *et al*., 1995), (Figure 1). *Tl* GluDH is most closely related in sequence, structure and stability to the latter and a structure based sequence alignment of the *Tl* GluDH against the more stable *Pf* enzyme, together with secondary structure assignments, is shown in Figure 2. Each subunit of the *Tl* enzyme is constructed from two domains, separated by a deep cleft. Domain I (residues 3-182 and 395-419) is responsible for directing the assembly of the subunits into a hexamer with 32 symmetry to give a molecule of cylindrical appearance and approximate dimensions 100 Å height and 80 Å diameter. With the exception of the C-terminal helix α14, which folds back onto domain I, the remaining residues (183-394) comprise domain II, the dinucleotide binding domain.

Across the wide variety of structures of GluDH that have been solved, differences of up to 18° in the relative orientation of the two domains have been observed. Even comparing different subunits within the asymmetric unit of specific crystal forms, differences of up to 11.9° in domain opening have been seen (Abeysinghe, 1993). For the three subunits in the asymmetric unit of the crystals of *Pf* GluDH, the two domains of the A and C subunits have domain openings, relative to the B subunit, of 0.9 and −0.6°, respectively. In the *Tl* GluDH crystals, a hexamer is present in the asymmetric unit and the relative domain openings of the six subunits, with respect to the B subunit of the *Pf* enzyme, vary between 0.5 and −3.7°.

Comparison of Tl and Pf GluDHs

Similarities in the overall fold and in the active site

Overall, the fold of *Tl* GluDH is almost identical with that of the more stable *Pf* enzyme and 205 and 211 α-carbon atoms of domains I and II can be superimposed with an rmsd of 0.59 and 0.38 Å, respectively. This close relationship in structure permits a detailed comparison of their three-dimensional structure to be made. The only region of significant structural difference is close to residue 209 in the *Pf* structure which lies in the loop between α6 and βg. The deletion of one residue of the *Tl* enzyme induces very localised changes in the structure at this position. Elsewhere, the percentage of residues in regular secondary structure for both enzymes is very similar (Table 1). The *Tl* enzyme appears to have a lower number of hydrogen bonds per residue than the more stable *Pf* enzyme, however this may just be a reflection of the lower resolution of the *Tl* enzyme structure.

The *B*-factors for the *Tl* structure are, in general, higher than those seen in *Pf* GluDH. However, a similar distribution of the *B*-factors for the two domains is seen between the two enzymes with the average *B*-factors for the hexamer of the *Tl* and *Pf* GluDH structures in domain I (43 and 32 Å^2, respectively) being lower than those in domain II (58 and 45 Å^2, respectively). Although the differences in *B*-factors between the two enzymes are significant and might be anticipated on account of their differences in thermal stability, they may just reflect the different crystal packing and the lower resolution of the *Tl* structure. Therefore, they cannot be attributed solely to differences in the thermal stability of the enzymes.

The assembly of the subunits into a hexamer in *Tl* GluDH is very similar to that seen in the *Pf*

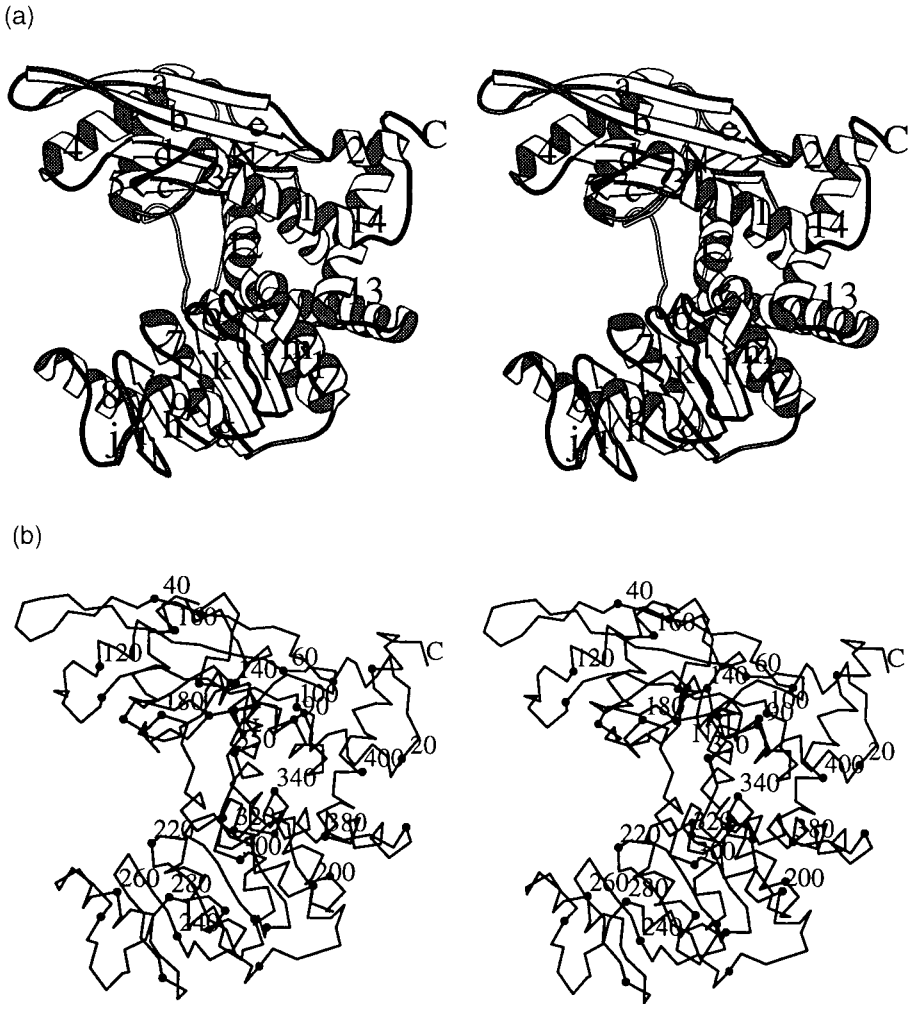

Figure 1. Stereo diagrams of a single subunit of *Tl* GluDH. The organisation of the subunit into two domains, separated by a deep cleft, can be seen. In this view, the 3-fold axis of the GluDH hexamer runs vertically with domain I lying uppermost and domain II in the lower portion of the Figure. (a) Schematic representation with strands (**a-m**) and helices (**1-14**) marked. (b) C^{α} trace with every tenth residue indicated by a black dot. The Figure was prepared using MOLSCRIPT (Kraulis, 1991).

enzyme. In both enzymes 3400 Å^2 of the 17,900 Å^2 of accessible surface (Lee & Richards, 1971) is buried per subunit.

Table 1. Comparison of the secondary structures of the GluDHs from *Pf* and *Tl*

	Pf	*Tl*
No. of residues per subunit	419	418
No. of residues in helical conformation (%)	208 (50)	199 (48)
No. of residues in β conformation (%)	66 (16)	76 (18)
No. of main-chain H bonds (% of total possible)	287 (68)	287 (69)
No. of intra-subunit protein-protein H bonds	578	561
No. of intersubunit protein-protein H bonds[a]	163	153
No. of protein-protein H bonds per residue	1.44	1.34

[a] This is the total for the hexamer.

The active site of GluDH has been identified from analysis of the binary complexes of *Cs* GluDH with NAD^+ and glutamate (Baker *et al.*, 1992; Stillman *et al.*, 1993). In this enzyme 21 residues have at least one atom lying within 6 Å of any atom of the glutamate substrate. All of these residues are identical in both the *Tl* and *Pf* enzymes, suggesting that the differential stability of these two GluDHs does not impose severe restrictions on the residues at the active site.

Effect of sequence changes between the two enzymes

In addition to the deletion, there are 52 other sequence differences between the *Pf* and *Tl* GluDHs (Figure 2). The differences in structure at these positions have been analysed in order to give further insights into the factors controlling stability.

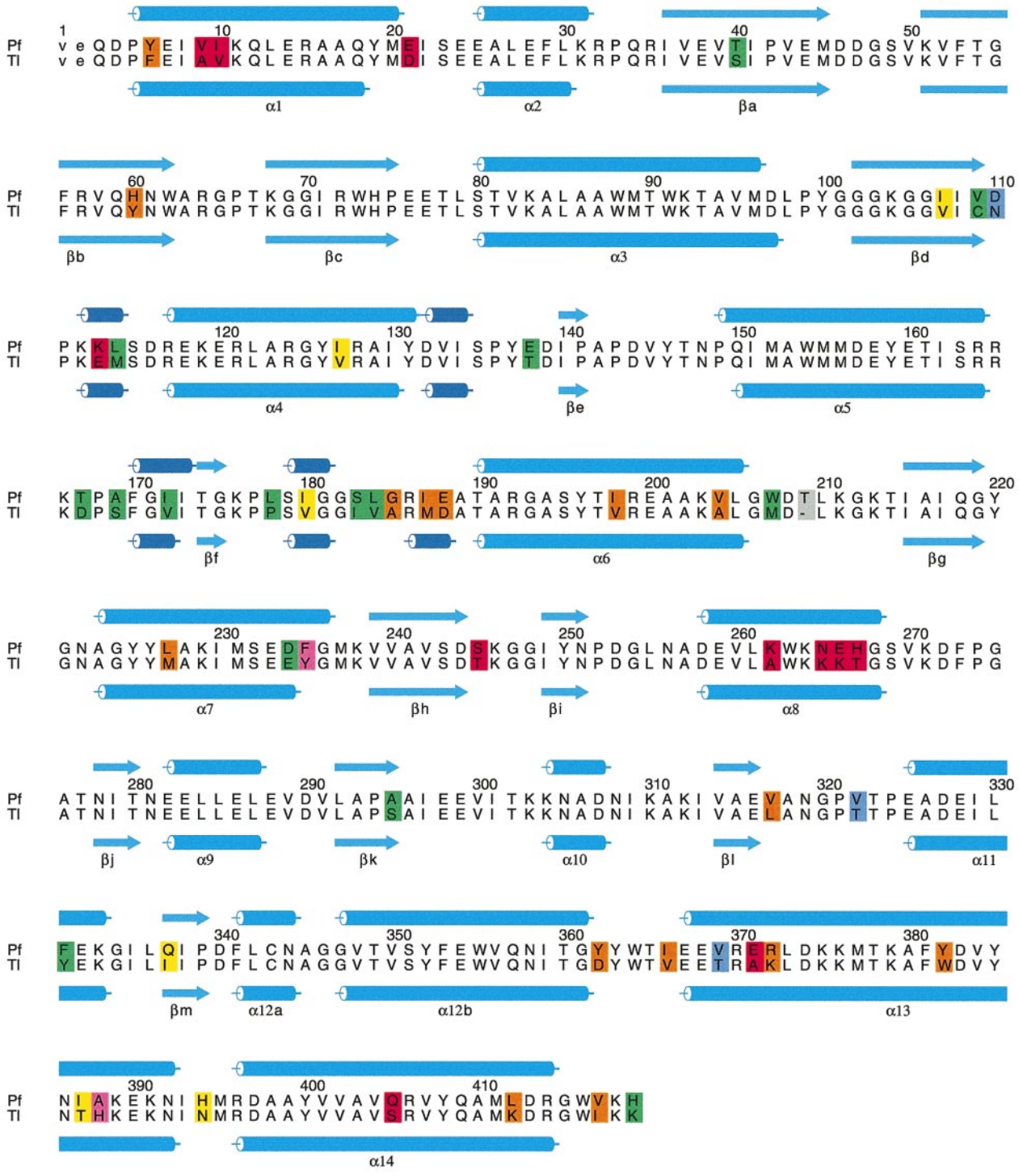

Figure 2. Alignment of the sequences for *Pf* and *Tl* GluDH. The amino acids for each sequence are identified by the single letter code, with those in lower case representing the N-terminal residues that are disordered in the X-ray structures of both GluDHs. The secondary structural elements of the three-dimensional structure of the two GluDHs are shown with α-helices represented by light blue cylinders, 3_{10} helices as dark blue cylinders and β-strands as arrows. The sequence numbering above refers to the *Pf* enzyme. The position of the single deletion between the two enzyme sequences is indicated by -. Residues highlighted in colour identify the 53 positions of sequence difference between the two GluDHs where each colour defines a different classification of sequence change: deletion (grey); partially disordered (red); complementary changes (orange); isosteric changes (blue); packing changes (yellow); those resulting in modification of the water structure (pink); those inducing main-chain or side-chain movements (green).

Changes between partially disordered residues

Five of the sequence differences between the two enzymes involve residues which are partially disordered in both structures (defined as having side-chain *B* factors >25 Å^2 above the average for the protein) and a further six of the sequence differences involve residues that are partially disordered in the *Pf* enzyme alone. Of these 11 residues, nine lie on the surface of the enzyme (defined as >30 % of the residue accessible to solvent). That these residues are disordered in both structures, or in just the structure of the more stable enzyme, leads us to suggest that they play little role in their differential thermal stability.

Complementary changes

Fifteen of the sequence differences occur not as isolated substitutions but rather are clustered in space (***Y6F*** and ***H60Y***; ***G185A*** and ***I366V***; ***I187M*** and ***E188D***; ***I198V***, ***L227M*** and ***V317L***; ***V204A*** and ***Y382W***; ***Y362D*** and ***R372K***; ***L412K*** and ***V417I***). The overall result of these changes maintains the packing within the structure and leads to no significant shifts in either neighbouring main-chain or side-chain elements. For example, Tyr6 and His60 pack against each other in the *Pf* GluDH structure and these are replaced by Phe6 and Tyr60, respectively in the *Tl* enzyme. Similarly, Ile198, Leu227 and Val317 pack in a local group in *Pf* GluDH, and these residues are replaced by Val198, Met227 and Leu318 in the *Tl* enzyme, to maintain the local packing (Figure 3(a)). Again, the extra space formed by the sequence change ***V204A*** in the *Tl* structure is filled by the side-chain of ***Y382W*** (Figure 3(b)).

Isosteric changes

In three cases an isosteric change occurs, maintaining the same local packing in both structures (***D110N***, ***V322T***, ***V369T***). In two of these cases a different pattern of hydrogen bonding is observed. Thus, a movement of the side-chain carboxyl of Glu315 together with the sequence change ***V322T*** results in a hydrogen bond between these two residues in the *Tl* GluDH structure (Figure 3(c)). Similarly, in the *Tl* enzyme, the side-chain hydroxyl of ***V369T*** is within hydrogen bonding distance of the main-chain carbonyl of Thr364. The isosteric substitution ***D110N***, maintains the same hydrogen bonding pattern at this position in the structure of the two enzymes with, in each case, a hydrogen bond formed between the side-chain residue OD1 and the main-chain amide nitrogen of K112.

Packing changes

Six of the changes involve the creation of five regions in buried parts of the *Tl* structure in which the packing appears less efficient. The single sequence changes ***I107V***, ***I127V***, ***I180V*** and ***I387T*** (Figure 3(d)) do not appear to introduce any significant movements of either main-chain or side-chain between the *Tl* and *Pf* enzymes, despite the addition of an extra methyl group at each position in the *Pf* enzyme. The other two residues are adjacent in the two structures (***Q337I*** and ***H394N***) and in the *Tl* GluDH adopt a different position from that seen in the *Pf* enzyme.

Changes resulting in modifications to the water structure

At a number of positions substitutions occur which involve a reorganisation of the local water structure. For example, residue 235 is phenylalanine in *Pf* GluDH, and is replaced by tyrosine in the *Tl* enzyme. Although at first glance this change might be expected to fill a cavity present in the *Pf* enzyme, in fact the extra hydroxyl group of the tyrosine side-chain in the *Tl* structure merely replaces an enzyme bound water molecule in the *Pf* structure, resulting in no significant overall change in packing. Similarly the sequence change ***A388H*** occurs in a surface depression in the *Pf* enzyme, which is occupied by enzyme bound water molecules. In the *Tl* enzyme the larger histidyl side-chain displaces these water molecules with no consequent overall change in packing.

Changes inducing main-chain or side-chain movements

The remaining 15 sequence differences (Figure 2) appear to result in subtle but distinct differences in the position and orientation of the main-chain and/or side-chain of neighbouring residues, with movements of the order of 0.5 Å. Although the resolution of the *Tl* structure is somewhat limited, the structural differences observed between this enzyme and the *Pf* GluDH are fully consistent with the observed sequence differences. For example, the replacement of isoleucine by valine at position 172 would, in the absence of other structural changes, lead to the production of a cavity adjacent to the main-chain between residues 134 and 137 in the *Tl* enzyme. Comparison of the two structures clearly reveals that in response to this substitution both main-chain and side-chain elements subtly rearrange so as to maximise the packing (Figure 4(a)). There are also a number of examples where a larger side-chain is present in the *Tl* structure and corresponding movements of the main-chain are necessary to accommodate the extra atoms (***T167D*** (Figure 4(b)), ***A169S***, ***A295S***).

For two of the substitutions complementary movements of adjacent side-chains occur. For example, Asp234 forms an ion pair with Arg192 in the *Pf* structure. This interaction is retained in the *Tl* enzyme, despite the sequence change ***D234E***, by a complementary movement of the side-chain of Arg192 (Figure 4(c)). For the change ***T40S***, the loss of the methyl group of the threonine in *Pf* is

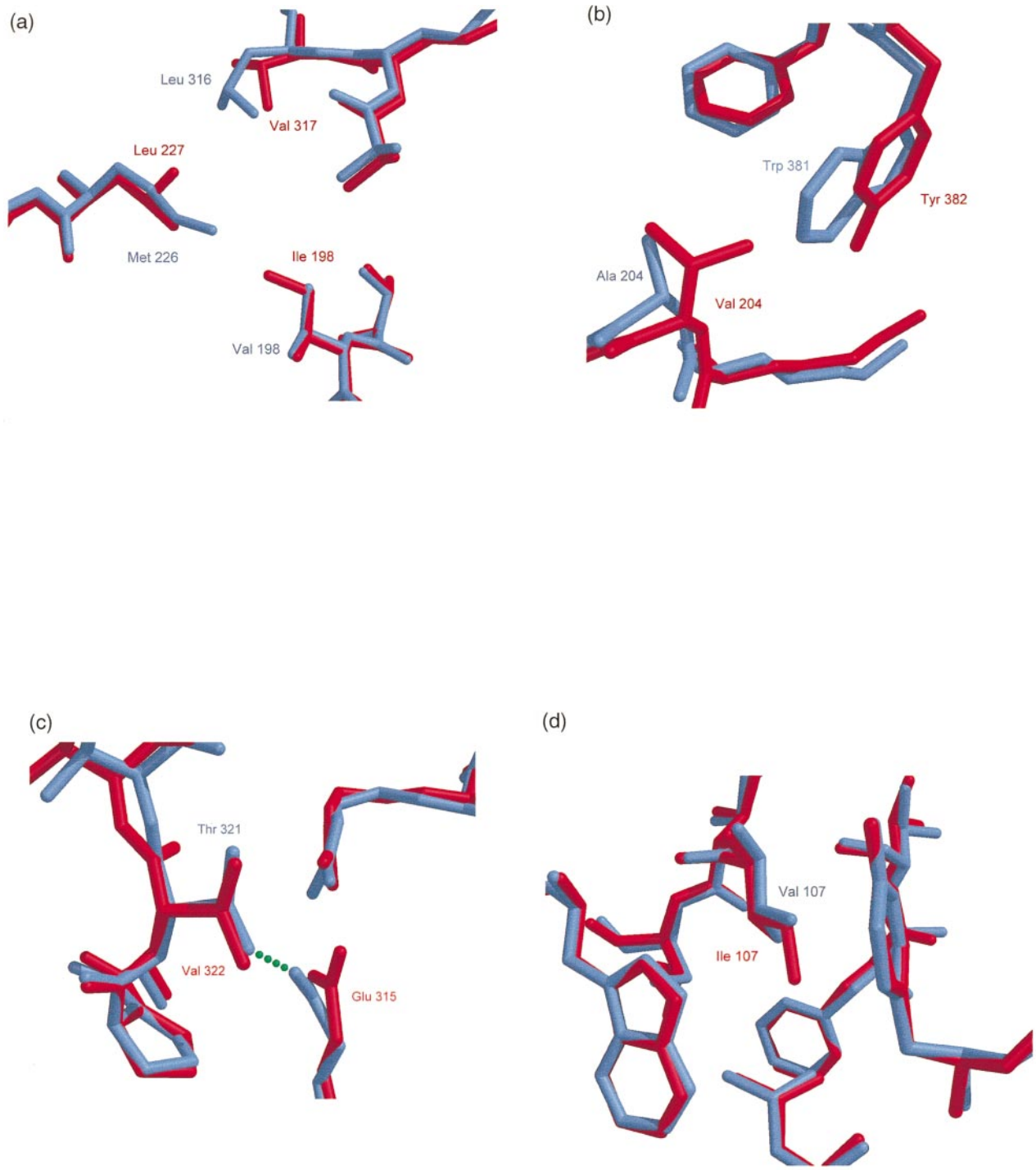

Figure 3. Diagrams of the superposition of the structures of the GluDHs from *Pf* (red) and *Tl* (blue) produced using the program MIDASPLUS (Ferrin *et al.*, 1988). Highlighting the local differences in structure between the two enzymes as a result of complementary sequence changes: (a) ***I198V***, ***L227M*** and ***V317L***; (b) ***V204A*** and ***Y382W***; (c) the isosteric sequence change ***V322T*** resulting in the formation of an extra hydrogen bond (green dotted line) in the *Tl* enzyme relative to the *Pf* GluDH; (d) the packing change ***I107V***.

compensated for by Val52 adopting a different rotamer in the *Tl* structure (Figure 4(d)).

Differences in ion pairs

Previous studies on the structure of *Pf* GluDH have shown that there is a substantial increase in both the number of ion pairs and the number of multi-centre ion pair networks compared to those observed in the equivalent mesophilic enzymes (Yip *et al.*, 1995). Such ion pair networks have also been observed in other hyperthermophilic proteins (Lim *et al.*, 1997; Russell *et al.*, 1997; DeDecker *et al.*,

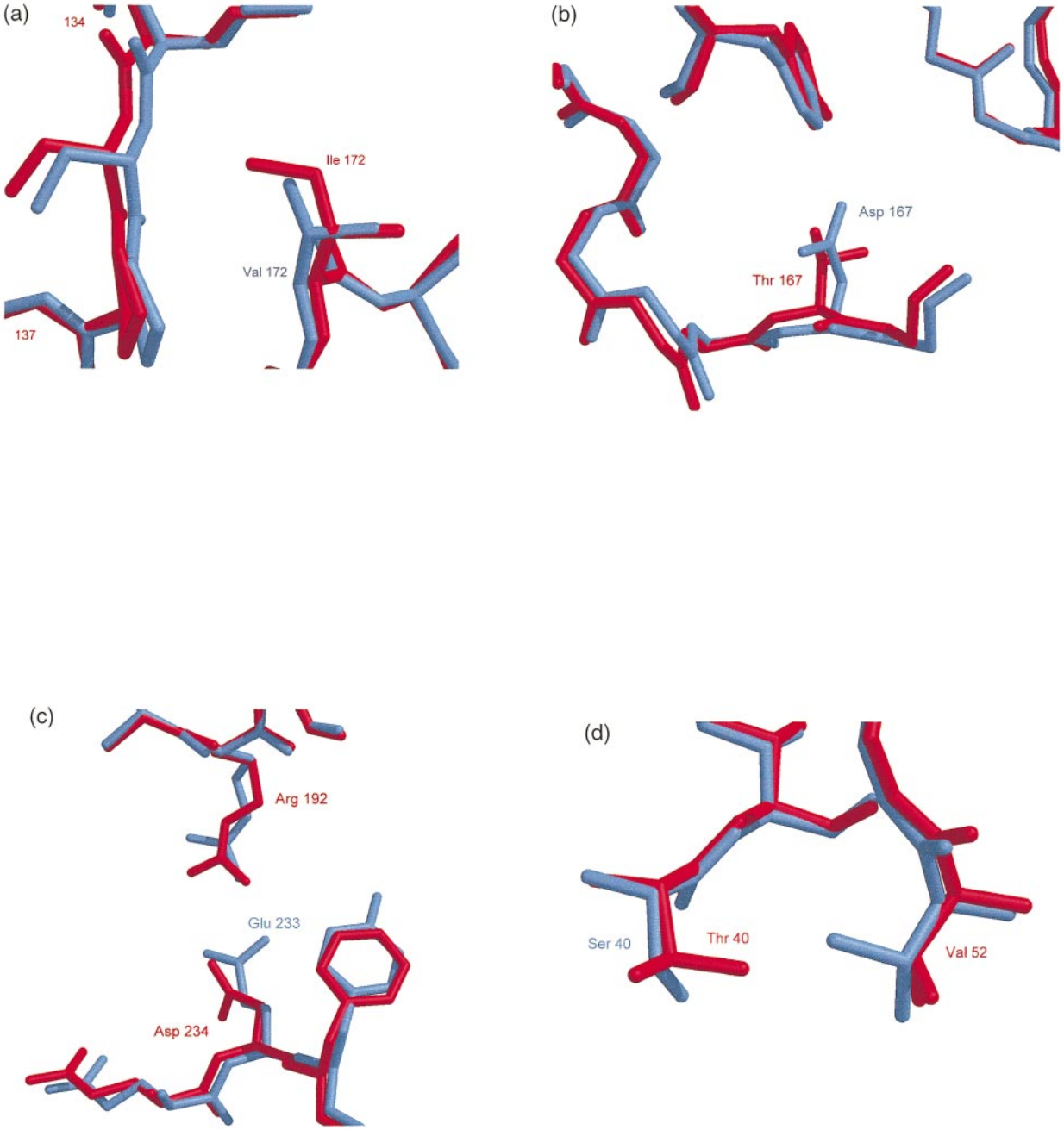

Figure 4. Diagram showing the local differences in structure between the *Pf* (red) and *Tl* (blue) GluDHs arising from sequence changes inducing main-chain and/or side-chain movements: (a) ***I172V***; (b) ***T167D***; (c) ***D234E***; (d) ***T40S***.

1996; Hennig *et al*., 1995) and have been suggested to enhance stability through the shared entropic costs upon ion pair formation (Nakamura, 1996). The most extensive ion pair network formed in the *Pf* enzyme involves the interaction of 18 residues located at the interface between four different subunits. Each of these residues is completely conserved in *Tl* GluDH, although two of the residues lying at the edge of the cluster (Arg117 and its 2-fold related partner) are more disordered in the *Tl* enzyme. Interestingly, a comparison of the ion pair interactions of *Thermotoga maritima* GluDH, an enzyme whose melting temperature (93 °C) is significantly less than that of either *Pf* or *Tl* GluDH, shows that in this enzyme the most extensive ion pair network is one of only seven residues (Knapp *et al*., 1997), suggesting that the size of the ion pair clusters may be important in determining stability.

The second largest ion pair network in the *Pf* enzyme involves six residues and is centred on Glu138, which makes three ion pair interactions to the side-chains of Arg35, Arg165 and Lys166 (Figure 5). Within the *Tl* structure, the ***E138T*** sequence change disrupts this ion pair network, with no other sequence substitutions restoring the lost ion pair interactions, as predicted by an earlier homology based modelling study (Yip *et al*., 1998). Thus the six residue cluster in *Pf* GluDH is

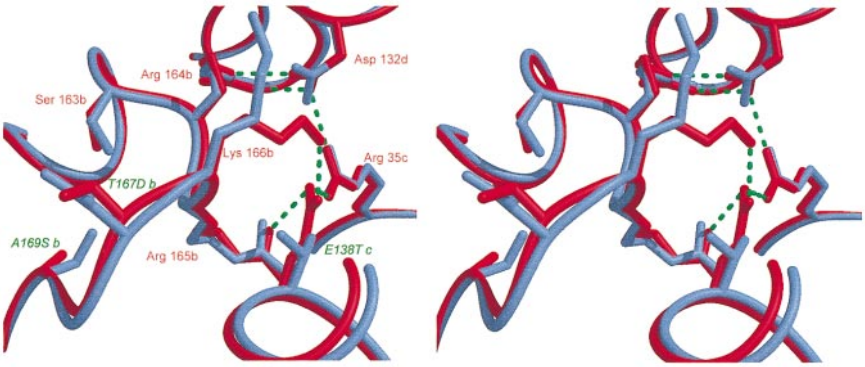

Figure 5. A stereo representation of the superposition between the *Pf* (red) and *Tl* (blue) GluDH structures displaying the main-chain of each as a smooth chain. Only the side-chains of the residues involved in the six residue ion pair cluster of *Pf* GluDH are highlighted, their equivalent side-chains in the *Tl* enzyme and the positions of neighbouring sequence changes in both enzymes are shown. Subtle displacement of the main-chain occurs with the two backbone loops of the *Pf* GluDH further apart at position 167.

replaced by one of only three residues in the *Tl* enzyme. Close examination of the two structures in this region also reveals subtle shifts in the relative positions of segments of main-chain including residues 164-168 as well as around position 138 itself (Figure 5).

In addition, the single ion pair interaction between His419 and Glu25 in *Pf* GluDH is lost in the *Tl* enzyme as a consequence of the sequence change ***H419K*** combined with an alternative conformation for the side-chain of Glu25.

Discussion

The comparison of the structure of *Tl* GluDH with that of the more stable *Pf* enzyme has highlighted a number of structural differences consistent with the current ideas on the mechanisms for thermal stability. Such analyses, however, are fraught with difficulties and we must be careful not to assume that all the sequence differences between *Tl* and *Pf* GluDHs are destabilising. Indeed, it is highly likely that some of the sequence changes between the two enzymes will stabilise the *Tl* structure, and the observed difference in stability is due to the balance of stabilising and destabilising interactions. For example, two of the isosteric changes, ***V322T*** and ***V369T*** introduce additional hydrogen bonds into the *Tl* structure compared to the situation seen in the *Pf* enzyme and the influence of these might well be stabilising.

Of the other structural differences seen between the *Pf* and *Tl* enzymes, the observation that the latter contains regions in which the packing appears less efficient is consistent with the idea that packing defects are destabilising (Kellis *et al*., 1989; Eriksson *et al*., 1992, 1993). Moreover, it is interesting to note that the sequence changes in three of these involve the exchange of isoleucine for valine with one occuring in a cluster of five isoleucine residues in the *Pf* enzyme. Such clusters of isoleucine residues have also been noted in the structure of *P. furiosus* citrate synthase (Russell *et al*., 1997). However, their role in conferring stability is as yet unknown.

During the catalytic cycle of enzymes belonging to the amino acid dehydrogenase superfamily, a change in the relative orientation of the enzyme's two domains occurs which is responsible for positioning the partners involved in hydride transfer into an appropriate orientation for catalysis (Stillman *et al*., 1993). This motion involves a large scale domain closure which is controlled by conformational changes at four hinge points in the structure (residues 181-187; 346-350; 362-365; and 392-393 inclusive). Interestingly, 12 (178, 180, 183, 184, 185, 187, 188, 362, 366, 387, 388, 394) of the 52 sequence differences between these two enzymes occur at, or near, the hinge regions (Baker *et al*., 1997). However, whether these sequence differences have any effect on the relative flexibility of the two domains, contributing to the ease with which this structural change is brought about, remains to be determined.

One of the major debates in the field of stability is the degree to which ion pairs can play a role in stabilising protein structures at high temperatures, where the hydrophobic interaction is enthalpy-driven rather than entropy-driven at mesophilic temperatures (Baldwin, 1986; Privalov & Gill, 1998; Perutz & Raidt, 1975). The comparison of the structures of the *Pf* and *Tl* GluDHs clearly reveals an overall decrease in the extent of the ion pair network formation (Table 2). In particular, the second largest ion pair network of six residues in *Pf* GluDH is not present in the *Tl* structure, due to the critical replacement of the central glutamate residue by threonine (***E138T***) (Figure 5). The question that arises, therefore, is whether this substitution is destabilising. In order to test this proposal a single mutation, T138E, was introduced into *Tl* GluDH with the aim of enhancing its stability. However, biochemical studies have established that this mutant enzyme is less stable, having a

Table 2. Comparison of ion pair interactions between *Pf* and *Tl* GluDHs

	Pf	*Tl*
No. of ion pairs per subunit (per residue)	45 (0.11)	38 (0.09)
% of charged residues forming ion pairs	54	36
% ion pairs formed by Arg/Lys/His	64/27/9	81/19/0
% ion pairs formed by Asp/Glu	47/53	52/48
% of all Arg forming ion pairs	90	90
No. of residues forming 2/3 ion pairs	17/5	11/5
No. of 2/3/4 residue networks[a]	54/24/12	48/24/12
No. of 5/6/18 residue networks[a]	12/6/3	Three 16-residue networks
% ion pairs in networks of >3 residues[a]	62	32
No. of intersubunit ion pairs[a]	54	54
No. of interdomain ion pairs	7	3

Ion pair interactions were identified using the criteria of Barlow & Thornton (1983).

[a] Comparisons of the ion pair networks and the number of intersubunit ion pairs refer to the number of such interactions in the hexamer.

melting temperature of 103.5 °C and a half life at 104 °C of <0.01 hour, compared to values of 109.0 °C and 0.3 hour for the wild-type enzyme, respectively (Vetriani *et al*., 1998). This result at first sight appears to undermine the idea that ion pairs play a role in conferring stability. However, as we have already noted, the local environment around position 138 in *Tl* GluDH is modified with respect to the *Pf* enzyme which arises from the differences in the side-chains at this and at neighbouring positions. These result in subtle positional shifts in the main-chain of the string of basic residues Arg164, Arg165, and Lys166, as well as in the main-chain of Thr138, each of which participate in the six residue ion pair network in *Pf* GluDH (Figure 5). In addition, other nearby sequence substitutions modify the context of the glutamate at position 138 in the T138E mutant of *Tl* GluDH, compared to the *Pf* enzyme. For example, the substitution ***T167D*** must necessarily modify the electrostatic potential at position 138 in the *Tl* enzyme. One possible consequence of the subtle position shifts is that the residues in the *Tl* GluDH may not necessarily be in the correct orientation to reproduce the ion pair cluster seen in the *Pf* enzyme and hence could explain why the single mutation T138E might not confer additional stabilisation. The analysis of a double mutant of *Tl* GluDH (T138E, D167T) shows that it has a substantially increased thermal stability compared to the wild-type *Tl* enzyme (melting temperature of the mutant is 111.5 °C and a half life at 104 °C of 1.1 hour (Vetriani *et al*., 1998)) whereas the control mutation, D167T, leads to a slight reduction in thermal stability, all measured at 0.5 M KCl. Thus, it is possible that in the double mutant the second mutation (D167T) works in conjunction with the first (T138E) to allow all the side-chains in the six residue ion pair network to be optimally aligned. Alternatively, we cannot rule out the possibility that unfavourable electrostatic contacts in the region of residue 138 arise when a glutamate is introduced at this position in the *Tl* enzyme, given that additional aspartic acid residue is present at position 167, even though the carboxyl group of the latter lies some 10 Å from the centre of the ion pair network. In support of this we note that at high salt concentrations (1 M KCl), the D167T mutation stabilises the *Tl* enzyme 2.5-fold relative to the wild-type (D.L.M., B. Lee & F.T.R., unpublished), suggesting that unfavourable electrostatic interactions may be shielded in high ionic strength solutions.

The related thermostable GluDH isolated from *Pyrococcus kodakaraensis* KOD1 also shows 90 % sequence identity to *Pf* GluDH and has a stability intermediate between the *Pf* and *Tl* enzyme but more closely related to that of the *Tl* GluDH. Examination of the sequence of the KOD1 GluDH shows that all the residues in the six residue ion pair network in *Pf* GluDH are conserved with the exception of the critical glutamate E138 which, as in the *Tl* enzyme, is replaced by threonine. In contrast to *Tl* GluDH, the T138E mutant of the KOD1 enzyme results in an increase in half-life at 100 °C from two hours for the wild-type recombinant enzyme to three hours in the mutant enzyme (Rahman *et al*., 1998). Analysis of the sequence of the KOD1 GluDH reveals that the residue at position 167 is glycine, distinct from that observed in *Pf* and *Tl* GluDHs. The loss of bulk at this position compared to the latter two enzymes may well be compensated by a further sequence change which introduces methionine at position 163 in place of serine in both of the other GluDHs (see Figure 5 for the relative position of these residues). Thus, the context of position 138 is again different in the *P. kodakaraensis* GluDH, potentially explaining the different behaviour of the single mutant T138E introduced into both KOD1 and *Tl* GluDHs.

The detailed understanding of the molecular basis of thermal stability of proteins has yet to emerge. Whilst a number of studies are suggesting a role for rigidifying mutations in controlling stability such analyses are not yet widely available and the view that multiple mechanisms can control stability still prevails. The detailed comparison of the two hyperthermophilic enzymes presented here is certainly suggestive of a role for ion pairs in control of stability. However, we also observe subtle changes in the context of specific residues between the two enzymes that arise from sequence differences. Given the marginal differences in stability between *Pf* and *Tl* GluDH the effect of these is very hard to predict. The comparison of two closely related structures however, has allowed us to focus our attention on distinct types of sequence changes which we can now follow up rationally in

a programme of site-directed mutagenesis. Whatever the outcome of that programme it is clear that stability data will need to be carefully correlated with the structural properties of the mutants before any unifying theme can be presented. In the long term, such detailed comparisons may test our ability to predict and calculate the properties of proteins and force us to re-examine strategies for molecular modelling and prediction of the effects of mutational changes.

Materials and Methods

Crystallisation

Tl GluDH was prepared as previously described (Ma *et al*., 1994) and stored at a concentration of 35-40 mg/ml in a buffer containing 50 mM Tris-HCl (pH 7.8), 2 mM DTT and 10 % (v/v) glycerol. For crystallisation, the protein solution was dialysed against a 40 mM Tris-HCl buffer (pH 8) to give a protein concentration of approximately 35 mg/ml. Crystals were grown using the hanging drop method of vapour diffusion by mixing 4 μl drops of the protein solution with equal portions of a precipitant solution made up of 0.1 M Hepes buffer (pH 8) containing 1.7-1.8 M ammonium sulphate and 1.5 % (w/v) PEG 8000. Crystals grew over a period of several months to reach a maximum dimension of 1.1 mm. These crystals were extremely sensitive to any changes in the mother liquor and hence could not be stabilised. Therefore, for crystallographic analysis they were mounted directly from the drop. The crystals belong to space group *C*2 with a hexamer in the asymmetric unit and have lattice constants $a = 141.9$ Å, $b = 197.5$ Å and $c = 125.7$ Å with $\beta = 113.6°$, and are distinct from those previously reported (Sedelnikova *et al*., 1996).

Data were collected at the CLRCC Daresbury Synchrotron Radiation Source on station PX 9.5 using X-rays with a wavelength of 0.92 Å, on crystals of the native enzyme to 2.5 Å and a mercury derivative, to 2.8 Å. The derivative was prepared by brushing solid grains of dimercuriacetate (DMA) onto a native crystal in a capillary tube and leaving overnight. In each case the data were collected using the rotation method with a 1.5° oscillation range. The data were processed with the MOSFLM package (Leslie, 1992) and scaled and merged with CCP4 software (CCP4, 1994) (Table 3).

A model of *Pf* GluDH (Yip *et al*., 1995) was used as a basis for a molecular replacement solution for the structure, but the initial map generated after the model was refined with the program TNT (Tronrud *et al*., 1987) was not of sufficient quality to confidently assign residues in regions of structural differences between the *Pf* and *Tl* enzymes. Therefore, in an attempt to provide a better initial phase set, the positions of the heavy atom sites in the DMA derivatives were obtained by difference Fourier methods using the phases provided by the molecular replacement solution. The heavy atom parameters were refined with the program MLPHARE (Otwinowski, 1991), which resulted in a phase set with an overall mean figure of merit of 0.35 to 2.8 Å resolution. Using a map derived from these phases, molecular masks were generated using MAMA (Kleywegt & Jones, 1993) and 200 cycles of solvent flattening and 6-fold molecular averaging were performed with the program DM (CCP4, 1994; Cowtan, 1994). The model was rebuilt from DM averaged phases and further refined using the refinement package TNT. Subsequent rebuilding was conducted by the examination of electron density maps based on coefficients $(2\ m|F_o| - D|F_c|)$ with combined isomorphous and calculated phases. The final model had a total of 416 residues built for each monomer, there being no electron density for the first two residues. The final *R*-factor for the model which comprises 19,542 non-hydrogen atoms with no added solvent is 0.192 for all data between 10 and 2.5 Å with an rmsd of 0.013 Å for bond lengths and 1.53° for bond angles ($R = \Sigma|(|F_{obs}| - |F_{calc}|)|/\Sigma(|F_{obs}|$, where $|F_{obs}|$ and $|F_{calc}|$ are the observed and calculated structure factor amplitudes, respectively). The corresponding free *R*-factor of 0.308 is somewhat higher, although the clear lack of bias in the refined electron density maps does not suggest that the structure is incorrect. The average *B*-factor for the hexamer is 46 Å^2 for main-chain atoms (50 Å^2 for side-chain atoms).

Table 3. X-ray data collection and phasing statistics

Data set	Native	DMA
Resolution (Å)	2.5	2.8
No. of observed reflections	173,711	89,463
No. of unique reflections	101,702	61,235
Completeness (%)	93	78
R_{merge} (%)[a]	4.2	6.3
Mean fractional isomorphous difference[b]		19.5
No. of heavy atom sites		6
Phasing power (acentric/centric)[c] (10-4.5 Å)		2.08/1.30
R_{cullis} (acentric/centric)[d] (10-4.5 Å)		0.61/0.62

DMA, dimercuriacetate.

[a] $R_{merge} = \Sigma_{hkl}|I_i - I_m|/\Sigma_{hkl}I_m$, where I_i and I_m are the observed intensity and mean intensity of related reflections, respectively.

[b] Mean fractional isomorphous difference $= \Sigma||F_{PH}| - |F_P|/\Sigma|F_P|$, where F_{PH} and F_P are the structure factor amplitudes for the derivative and native crystals repectively.

[c] Phasing power $= \langle F_H/\text{lack of closure}\rangle$.

[d] $R_{cullis} = \langle\text{lack of closure}\rangle/\langle\text{isomorphous difference}\rangle$.

PDB accession numbers

The co-ordinates for *Tl* GluDH have been submitted to the Brookhaven Data Protein Bank (entry code 1BVU).

Acknowledgements

We thank the support staff at the Synchrotron Radiation Source at CLRC Daresbury Laboratory for assistance with station alignment. This work was supported by grants from the EU, BBSRC and NEDO to D.W.R., the National Science Foundation, US Department of Energy and the Knut and Alice Wallenberg Foundation (ATP program) to F.T.R. and the National Sciences Foundation to M.W.W.A. The Krebs Institute is a designated BBSRC Biomolecular Science Centre and a member of the North of England Structural Biology Centre.

References

Abeysinghe, I. S. B. (1993). Structural studies on the $NADP^+$-linked glutamate dehydrogenase from *E. coli*. PhD thesis, University of Sheffield.

Baker, P. J., Britton, K. L., Engel, P. C., Farrants, G. W., Lilley, K. S., Rice, D. W. & Stillman, T. J. (1992). Subunit assembly and active site location in the structure of glutamate dehydrogenase. *Proteins: Struct. Funct. Genet.* **12**, 75-86.

Baker, P. J., Waugh, M. L., Wang, X-G., Stillman, T. J., Turnbull, A. P., Engel, P. C. & Rice, D. W. (1997). Determinants of substrate specificity in the superfamily of amino acid dehydrogenases. *Biochemistry,* **36**, 16109-16115.

Baldwin, R. L. (1986). Temperature dependence of the hydrophobic interaction in protein folding. *Proc. Natl Acad. Sci. USA,* **83**, 8069-8072.

Barlow, D. J. & Thornton, J. M. (1983). Ion-pairs in proteins. *J. Mol. Biol.* **168**, 857-885.

Bogin, O., Peretz, M., Hacham, Y., Korkhin, Y., Frolow, F., Kalb, A. J. & Burstein, Y. (1998). Enhanced thermal stability of *Clostridium beijerinckii* alcohol dehydrogenase after strategic substitution of amino acid residues with prolines from the homologous thermophilic *Thermoanaerobacter brockii* alcohol dehydrogenase. *Protein Sci.* **7**, 1156-1163.

CCP4, (1994). The CCP4 Suite: programs for protein crystallography. *Acta Crystallog. sect. D,* **50**, 760-763.

Chan, M. K., Mukand, S., Kletzin, A., Adams, M. W. & Rees, D. C. (1995). Structure of a hyperthermophilic tungstopterin enzyme, aldehyde ferredoxin oxidoreductase. *Science,* **267**, 1463-1469.

Cowtan, K. (1994). DM: An automated procedure for phase improvement by density modification. In *Joint CCP4 and ESF-EACBM Newsletter on Protein crystallography*, vol. 31, pp. 34-38, SERC Daresbury Laboratory, UK.

DeDecker, B. S., O'Brien, R., Fleming, P. J., Geiger, J. H., Jackson, S. P. & Sigler, P. B. (1996). The crystal structure of a hyperthermophilic archaeal TATA-box binding protein. *J. Mol. Biol.* **264**, 1072-1084.

Elcock, A. H. (1998). The stability of salt bridges at high temperatures: implications for hyperthermophilic proteins. *J. Mol. Biol.* **284**, 489-502.

Eriksson, A. E., Baase, W. A., Zhang, X., Heinz, D. W., Blaber, M., Baldwin, E. P. & Matthews, B. W. (1992). Response of a protein structure to cavity-creating mutations and its relation to the hydrophobic effect. *Science,* **255**, 178-183.

Eriksson, A. E., Baase, W. A. & Matthews, B. W. (1993). Similar hydrophobic replacements of Leu99 and Phe153 within the core of T4 lysozyme have different structural and thermodynamic consequences. *J. Mol. Biol.* **229**, 747-769.

Ferrin, T. E., Huang, C. C., Jarvis, L. E. & Langridge, R. (1988). The MIDAS display system. *J. Mol. Graph.* **6**, 13-27.

Fiala, G. & Stetter, K. O. (1986). *Pyrococcus furiosus* sp. *nov* represents a novel genus of marine heterotrophic archaebacteria growing optimally at 100 °C. *Arch. Microbiol.* **145**, 56-61.

Flam, F. (1994). The chemistry of life at the margins. *Science,* **265**, 471-472.

Hennig, M., Darimont, B., Sterner, R., Kirschner, K. & Jansonius, J. N. (1995). 2.0 Å structure of indole-3-glycerol phosphate synthase from the hyperthermophile *Sulfolobus solfataricus*: possible determinants of protein stability. *Structure,* **3**, 1295-1306.

Jaenicke, R. (1996). Stability and folding of ultrastable proteins: eye lens crystallins and enzymes from thermophiles. *FASEB J.* **10**, 84-92.

Kellis, J. T., Nyberg, K. & Fersht, A. R. (1989). Energetics of complementary sidechain packing in a protein hydrophobic core. *Biochemistry,* **28**, 4914-4922.

Kleywegt, G. J. & Jones, T. A. (1993). Masks made easy. In *CCP4 and ESF-EACBM Newsletter on Protein Crystallography*, vol. 28, pp. 56-59, SERC Daresbury Laboratory, UK.

Knapp, S., de Vos, W., Rice, D. W. & Ladenstein, R. (1997). Crystal structure of glutamate dehydrogenase from the hyperthermophilic eubacterium *Thermotoga maritimia* at 3.0 Å resolution. *J. Mol. Biol.* **267**, 916-932.

Korndörfer, I., Steipe, B., Huber, R., Tomschy, A. & Jaenicke, R. (1995). The crystal structure of holo-glyceraldehyde-3-phosphate dehydrogenase from the hyperthermophilic bacterium *Thermotoga maritima* at 2.5 Å resolution. *J. Mol. Biol.* **246**, 511-521.

Kraulis, P. J. (1991). MOLSCRIPT: a program to produce both detailed and schematic plots of protein structures. *J. Appl. Crystallog.* **24**, 946-950.

Lee, B. & Richards, F. M. (1971). The interpretation of protein structures: estimation of static accessibility. *J. Mol. Biol.* **55**, 379-400.

Leslie, A. G. W. (1992). Recent changes to the MOSFLM package for film processing and image plate data. In *Joint CCP4 and ESF-EACBM Newsletter on Protein Crystallography*, no. 26, SERC Daresbury Laboratory, UK.

Lim, J.-H., Yu, Y. G., Han, Y. S., Cho, S. J., Ahn, B. Y., Kim, S. H. & Cho, Y. J. (1997). The crystal structure of an Fe-superoxide dismutase from the hyperthermophile *Aquifex pyrophilus* at 1.9 Å resolution: structural basis for thermostability. *J. Mol. Biol.* **270**, 259-274.

Ma, K., Robb, F. T. & Adams, M. W. W. (1994). Purification and characterisation of NADP-specific alcohol dehydrogenase and glutamate dehyrogenase from the hyperthermophilic archaeon *Thermococcus litoralis*. *Appl. Environ. Microbiol.* **60**, 562-568.

Nakamura, H. (1996). Roles of electrostatic interaction in proteins. *Quart. Rev. Biophys.* **29**, 1-90.

Neuner, A., Jannasch, H. W., Belkin, S. & Stetter, K. O. (1990). *Thermococcus litoralis* sp *nov*-a new species of extremely thermophilic marine. *Arch. Microbiol.* **153**, 205-207.

Otwinowski, Z. (1991). Maximum likelihood refinement of heavy atom parameters. In *Proceedings of the CCP4 Study Weekend: Isomorphous Replacement and Anomalous Scattering DL/SCI/R32* (Wolf, W., Evans, P. R. & Leslie, A. G. W., eds), pp. 80-86, SERC Laboratory, Daresbury, Warrington, UK.

Perutz, M. F. & Raidt, H. (1975). Stereochemical basis of heat stability in bacterial ferredoxins and in haemoglobin A2. *Nature,* **255**, 256-259.

Privalov, P. L. & Gill, S. J. (1998). Stability of protein structure and hydrophobic interaction. *Advan. Protein. Chem.* **39**, 191-234.

Rahman, R. N. Z. A., Fujiwara, S., Nakamura, H., Takagi, M. & Imanaka, T. (1998). Ion pairs involved in maintaining a thermostable structure of glutamate dehydrogenase from a hyperthermophilic archaeon. *Biochem. Biophys. Res. Commun.* **248**, 920-926.

Russell, R. J. M., Hough, D. W., Danson, M. J. & Taylor, G. L. (1994). The crystal structure of citrate synthase

from the thermophilic archaeon, *Thermoplasma acidophilum*. *Structure,* **2**, 1157-1167.

Russell, R. J. M., Ferguson, J. M. C., Hough, D. W., Danson, M. J. & Taylor, G. L. (1997). The crystal structure of citrate synthase from the hyperthermophilic archaeon *Pyrococcus furiosus* at 1.9 Å resolution. *Biochemistry,* **36**, 9983-9994.

Sedelnikova, S. E., Yip, K. S. P., Stillman, T. J., Ma, K., Adams, M. W., Robb, F. T. & Rice, D. W. (1996). Crystallisation of the glutamate dehydrogenase from the hyperthermophilic archaeon *Thermococcus litoralis*. *Acta Crystallog. sect. D,* **52**, 1185-1187.

Starich, M. R., Sandman, K., Reeve, J. N. & Summers, F. (1996). X-ray crystal structures of the oxidised and reduced forms of the rubredoxin from the marine hyperthermophilic archaebacterium *Pyrococcus furiosus*. *J. Mol. Biol.* **255**, 187-203.

Stillman, T. J., Baker, P. J., Britton, K. L. & Rice, D. W. (1993). Conformational flexibility in glutamate dehydrogenase. Role of water in substrate recognition. *J. Mol. Biol.* **234**, 1131-1139.

Tanner, J. J., Hecht, R. M. & Krause, K. L. (1996). Determinants of enzyme thermostability observed in the molecular structure of *Thermus aquaticus* D-glyceraldehyde-3-phosphate dehydrogenase at 2.5 Å resolution. *Biochemistry,* **35**, 2597-2609.

Tronrud, D. E., Ten, Eyck L. F. & Matthews, B. W. (1987). An efficient general purpose least squares refinement program for macromolecular structures. *Acta Crystallog. sect. A,* **43**, 489-501.

Van Den Berg, B., Vriend, G., Veltman, O. R. & Eijsink, V. G. H. (1998). Engineering an enzyme to resist boiling. *Proc. Natl Acad. Sci. USA,* **95**, 2056-2060.

Vetriani, C., Maeder, D. L., Tolliday, N., Yip, K. S-P., Stillman, T. J., Britton, K. L., Rice, D. W., Klump, H. H. & Robb, F. T. (1998). Protein thermostability above 100 °C: a role for ionic interactions. *Proc. Natl Acad. Sci. USA,* **95**, 12300-12305.

Vogt, G., Woell, S. & Argos, P. (1997). Protein thermal stability, hydrogen bonds, and ion pairs. *J. Mol. Biol.* **269**, 631-643.

Yip, K. S. P., Stillman, T. J., Britton, K. L., Artymiuk, P. J., Baker, P. J., Sedelnikova, S. E., Engel, P. C., Pasquo, A., Chiaraluce, R., Consalvi, V., Scandurra, R. & Rice, D. W. (1995). The structure of *Pyrococcus furiosus* glutamate dehydrogenase reveals a key role for ion-pair networks in maintaining enzyme stability at extreme temperatures. *Structure,* **3**, 1147-1158.

Yip, K. S. P., Britton, K. L., Stillman, T. J., Lebbink, J., de Vos, W. M., Robb, F. T., Vetriani, C., Maeder, D. & Rice, D. W. (1998). Insights into the molecular basis of thermal stability from the analysis of ion-pair networks in the glutamate dehydrogenase family. *Eur. J. Biochem.* **255**, 336-346.

Zhang, X. J., Baase, W. A., Schoichet, B. K., Wilson, K. P. & Matthews, B. W. (1995). Enhancement of protein stability by the combination of point mutations in T4 lysozyme is additive. *Protein Eng.* **8**, 1017-1022.

Edited by R. Huber

(Received 17 June 1999; received in revised form 15 September 1999; accepted 15 September 1999)